The Influence of Long-Range Surface Forces on the Contact Angle of Nanometric Droplets and Bubbles

Antonio Stocco, H. Moehwald

Published in final edited form as:
Stocco, A., & Möhwald, H. (2015). The influence of long-range surface forces on the contact angle of nanometric droplets and bubbles. *Langmuir, 31*(43), 11835-11841. doi:10.1021/acs.langmuir.5b02922.

The influence of long-range surface forces on the contact angle of nanometric droplets and bubbles

Abstract

For a droplet or a bubble of dimensions below 100 nm, long-range surface forces such as long-range van der Waals forces can compete with capillarity, which leads to a size dependence of the contact angle. This is discussed in this work, where we also show that the effect cannot simply be described by a normalized line tension. We calculate interfacial profiles for typical values of van der Waals forces and discuss the role of long-range surface forces on the contact angle of nanobubbles and nanodrops.

The influence of long-range surface forces on the contact angle of nanometric droplets and bubbles

Antonio Stocco,[1,2*] *Helmuth Möhwald*[3]

[1]Laboratoire Charles Coulomb (L2C), UMR 5221 CNRS-University of Montpellier, Montpellier F-34095, France.

[2]DWI − Leibniz-Institut für Interaktive Materialien, Aachen 52056, Germany.

[3]Max Planck Institute of Colloids and Interfaces, Potsdam 14476, Germany

*corresponding author: antonio.stocco@umontpellier.fr

KEYWORDS

Nanodrops, nanobubbles, contact angle, long-range surface forces, line tension

ABSTRACT. For a droplet or a bubble of dimensions below 100 nm long-range surface forces such as long range van der Waals forces can compete with capillarity, which leads to a size dependence of the contact angle. This is discussed in this work, where we also show that the effect cannot simply be described by a normalized line tension. We calculate interfacial profiles for typical values of van der Waals forces and discuss the role of long-range surface forces on the contact angle of nanobubbles and nanodrops.

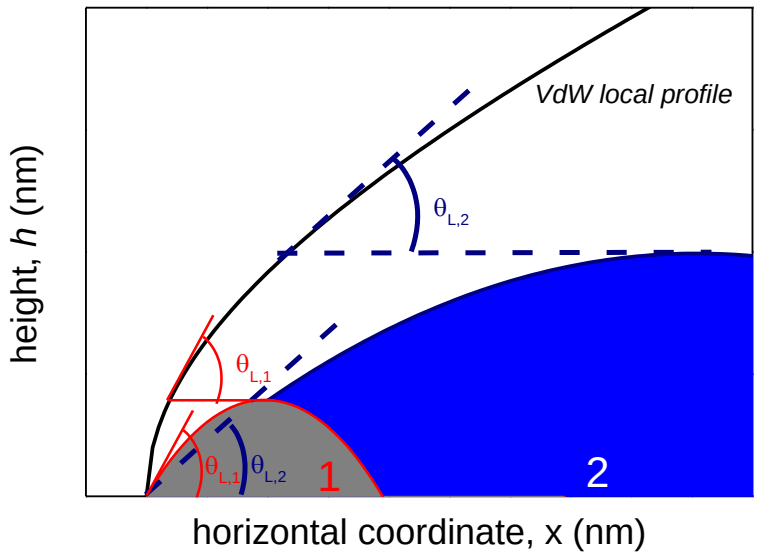

1. INTRODUCTION

Wetting at the nanoscale is a most relevant field of fundamental research and applications. Nanobubbles play key roles for the control of interfacial friction and for the propulsion

mechanism of some artificial microswimmers.[1,2] Nanosized liquid drops are also important in microelectronics, microfluidics and are relevant for biomedical coatings and textile processes.[3]

At length scales between a nanometer and a micron, long-range surface forces play a key role for the equilibrium states of a given multiphase system. Such forces include long range Van der Waals, electrostatic, hydrophobic and hydration interactions. Hydrophobic interactions refer to the attraction manifested between two hydrophobic media in water.[4] Hydration interactions (1-2 nm range) are repulsive solvation forces observed, when two hydrophilic interfaces approach. The nature of the observed repulsion is connected to the strong binding of water at the interface and the formation of hydrogen bonding networks, which act against the approach of the two interfaces.[5] Only Van der Waals, electrostatic and structural interactions are usually included in the Derjaguin disjoining pressure,[6] even if other interactions such as double layer electrostatic and long range hydrophobic interactions act on the same length scales.[4]

If the system under consideration is composed of two fluids and a solid, an equilibrium state can be described by partial wetting, where a drop or a bubble adopts a shape which minimizes the interactions at play. If the solid is a planar substrate, a drop tends to minimize its interfacial energy which leads to a spherical cap shape, if the drop dimension is smaller than few millimeters and gravity can be neglected. The spherical cap shape is found in many experiments for drops and bubbles sitting on smooth and clean substrates even when their dimensions become micrometric or even smaller.[7,8,9,10] In any case, for millimetric, micrometric or submicrometric drops, the interfacial profile deviates from the spherical cap shape close to the triple line at the nanoscale. This is expected since capillarity competes with long-range surface forces, which eventually dominate for distances close to few nanometers.[11] This deviation of the profile may be neglected for macroscopic bubbles or drops, since it represents only a negligible part of the

profile. However, this is not the case for nanometric drops and bubbles, for which long-range surface forces play a central role in the statics and dynamics of wetting.

Some recent investigations have been focused on the formation and stability of nanobubbles, which are observed mostly on hydrophobic surfaces immersed in a liquid. Nanobubbles possess heights lower than 100 nm and in many experiments they are found to be very stable.[2,9,10,12,13] This long time stability is somewhat surprising and many theoretical models attempted to quantify the experimental observations. Recently, an explanation based on contact line pinning and gas oversaturation of the liquid, which balance the gas diffusion driven by the Laplace pressure, has been proposed.[14,15] Line tension, collective diffusion effects have been also discussed in the literature to explain some aspects of the stability and the contact angle of nanobubbles.[2,16,17] One remarkable feature is also represented by the difference in contact angle between those nanobubbles and the corresponding macroscopic air bubbles. However, some questions such as the value of the capillary pressure inside the nanobubbles and the role of surface forces on the contact angle remain open,[2,10,16,18] and the desirable control on the formation and stability of nanobubbles is not yet fully achieved, which represents a major drawback for applications.

Many issues related to the physics of surface nanobubbles are common to the physics of surface nanodrops.[14] Also for nano-sized drops, line tension is usually invoked to describe the contact angle of droplets of decreasing sizes. In many experiments the droplet height can be as small as few nanometers. Negative values of the line tension have been found in most of the experiments.[6,7,16] Negative line tension values would imply that drops are not stable, since the increase of the contact line perimeter results in a decrease of the total energy of the system. This

is in contrast to the experimental observations which attest a long time stability of those nanodrops.

In this contribution, we recall the importance of long-range surface forces (which are usually neglected in the recent literature) on the shape of nanometric droplets and bubbles. The focus is on Van der Waals interactions and on the interfacial profiles and contact angles of nanometric drops and bubbles. We expect that the long range nature of the forces affects the domain shape especially near the triple line and consider this in a quantitative way.

Section 2 and 3 provide a theoretical background on contact angle and line tension. Motivation of this work and related key problems are presented in section 4. Interfacial profile results and discussion (section 5 and 6) are followed by the summary and perspectives.

2. CONTACT ANGLE

The equilibrium contact angle of a sessile drop on a solid substrate in partial wetting is defined in the far-field, where the minimum energetic state leads to a spherical cap profile of the drop. Zooming on the triple line region where the three phases meet, one finds that the droplet profile deviates from a spherical cap due to long-range surface forces originating from the physicochemical properties of the media, see Fig. 1.

Despite the fact that the local contact angle θ_L in the colloidal region of a drop is different from a macroscopic contact angle, an equilibrium contact angle θ_E can be always defined by considering that in the far field any local change (down to the molecular scale) will not affect the calculation of a free energy balance, if the triple line is simply shifted by an infinitesimal distance.[11]

The equilibrium of interfacial energies for a solid (S)-vapour (V)- liquid (L) system can be expressed in terms of the work associated with an incremental area change $l\mathrm{d}x$ on the solid substrate, see Fig. 1:[11]

$$W_{II\text{-}I} = \sigma_{SV}\, l\mathrm{d}x - \sigma_{SL}\, l\mathrm{d}x - \gamma\, l\mathrm{d}x \cos\theta_E = 0 \qquad \text{Eq. 1}$$

where σ_{SV}, σ_{SL} and γ are the solid-vapour, solid-liquid and liquid-vapour interfacial tensions, respectively. In Eq. 1 it is also assumed that local contact angles in the colloidal region simply translate when shifted by $\mathrm{d}x$. Note that we define x = 0 at the place where the spherical cap profile touches the solid substrate.

The Young-Laplace equation is obtained from eq. 1 :

$$\cos\theta_E = (\sigma_{SV} - \sigma_{SL}) / \gamma. \qquad \text{Eq. 2}$$

Hence, without accounting for a line tension contribution, it is possible to describe an equilibrium contact angle in the far-field, being aware that in the colloidal region the local profile may be very different from the far field profile, i.e. for distances $< \approx 1$ μm. The latter distance describes the limit, for which long-range surface forces become negligible compared to capillary forces.

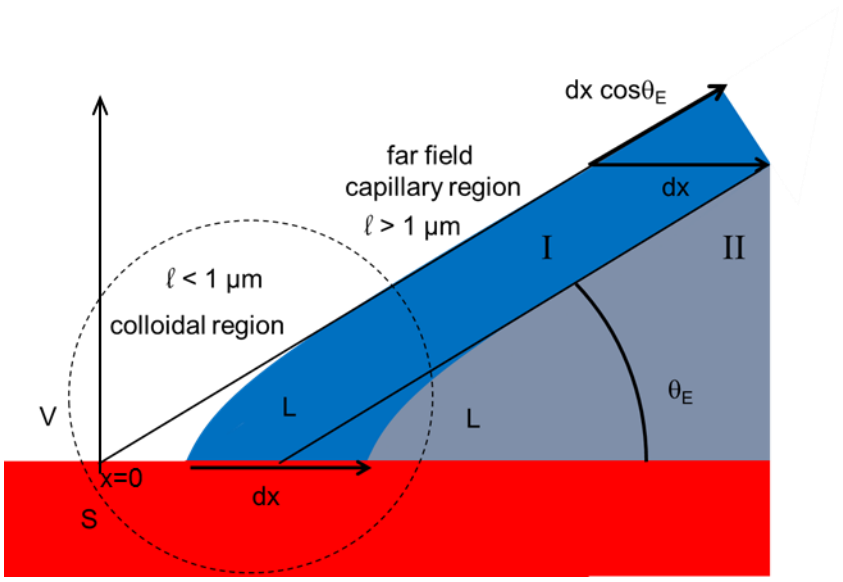

Figure 1. Sketch of a droplet profile in the colloidal region for characteristic length scales lower than a micrometer and in the far field region. Upon a shift dx of the triple line, one can always define an equilibrium contact angle accounting only for interfacial energy contributions. x = 0 at the place where the spherical cap profile touches the solid substrate.

Different theoretical approaches aimed at describing the interface profile at small scales.[20] Long-range surface forces, line tension and contact angle hysteresis have been discussed for the interface profile of macroscopic drops.[20,21]

3. LINE TENSION

Considering that in partial wetting three bulk phases form three interfaces and a common contact line, a thermodynamic equilibrium can be described in the far field accounting both for three interfacial tension and a line tension terms. The latter is associated to the energy contribution of the triple line. Line tension can be regarded as the leading term of the total macroscopic free energy of the system after subtracting contributions proportional to volume and interface.[22] Two

different sources of excess energy are related to the line tension. On a molecular level, the intermolecular interactions between two media will be affected by the presence of the third one on the triple line, leading to an unsaturation of interactions.[23] The second source of excess energy is related to the interface profile disturbed by long-range surface forces which tend to bend a spherical cap profile in order to minimize the local energy of the system.[23]

However, it is non trivial to calculate and measure the line tension according to the previous definition. One way to evaluate the line tension contribution is to find the microscopic profile of a partially wetting drop and consider the energy associated with the deviation between the microscopic profile and the macroscopic spherical cap profile.[22] Within this approach, the line tension is a constant calculated by the effective interfacial potential for the solid liquid vapour system accounting for three terms: (i) the asymptote of the profile at the contact line (ii), the whole interfacial profile and the corresponding local effective interface potential, (iii) and the interactions between fluid molecules.[22] From these calculations one finds the theoretical line tension for a given system which can be compared to the experimental line tension measured from contact angle experiments performed on droplets or bubbles of different sizes.[7,18,24] Note that in this description the drop dimension is macroscopic, but only the microscopic profile (for characteristic length scale smaller than a micrometer) is relevant for the line tension calculation.[24]

The line tension has also an effect on the equilibrium contact angle. This is apparently in contrast with the definition of the equilibrium contact angle described in the previous section where an equilibrium contact angle can be always defined in the far field (see Fig. 1).

A reconciliation between these descriptions could be done accounting for a change of the local interfacial profile upon an infinitesimal translation and introducing a line energy contribution kdl in Eq. 1:[23]

$$\sigma_{SV}\, l\mathrm{d}x - \sigma_{SL}\, l\mathrm{d}x - \gamma\, l\mathrm{d}x \cos\Theta - k\mathrm{d}l = 0 \qquad \text{Eq. 3}$$

However, it is worth noting that even if the interfacial profile simply translates (Fig. 1), one could always write equation 3 and associate the line energy term to a cohesive excess energy of the three phase system analogously as one considers the interfacial tension for a two phase system.

From equation 3, a far field equilibrium contact angle accounting for a line tension term could be defined:

$$\sigma_{SV} = \sigma_{SL} + \gamma \cos\Theta + k\, \mathrm{d}l/(l\mathrm{d}x)$$

$$\cos\Theta = \cos\theta_E - (k/\gamma)\, \mathrm{d}l/(l\mathrm{d}x) \qquad \text{Eq. 4}$$

Θ is the equilibrium contact angle that accounts also for the line energy contribution; whilst, θ_E accounts only for interfacial tensions. Note that for a drop wetting a planar solid, $\mathrm{d}l = 2\pi(R_d+\mathrm{d}x) - 2\pi R_d = 2\pi\mathrm{d}x$ (where R_d is the droplet contact radius) and $\mathrm{d}l/(l\mathrm{d}x) = 1/R_d$ is the curvature of the contact line. Hence Eq.4 becomes:[23]

$$\cos\Theta = \cos\theta_E - k/(\gamma R_d). \qquad \text{Eq. 5}$$

The modified Young-Laplace equation describes as well a far field balance of surface forces where an additional term, the line tension, is introduced. Note that Θ depends on the droplet size R_d. From eq. 5, the linear dependence of the cosine of the contact angle on the inverse of the

droplet size was used to calculate the line tension. Within the resolution of the experiments the drop/bubble shapes were found always spherical cap like even for drops/bubbles of nanometric sizes. Analysis of the experimental data was carried out within the modified Young-Laplace equation and in most of the cases a linear fit of the cosine of the contact angle versus the inverse of the drop size was imposed to evaluate the line tension.[7,8,18]

The way equation 2 and 5 are derived implies that drop or bubble dimensions extend to the far field.

4. KEY PROBLEM OF THIS WORK

Now we ask the following questions: Can we predict the interfacial profile when the drop/bubble dimensions extend only in the colloidal region (i.e. dimensions smaller than a micrometer)? Can the spherical cap profile of submicrometric drops/bubbles be set by the far field equilibrium contact angle accounting or not for a line tension? What is the role of the local contact angle defined in the colloidal region?

We show in Fig 2 that for a 2 μm radius droplet, the spherical cap profile merges a local interfacial profile for a distance of the order of 0.1 μm (5 % of the radius). Hence, the droplet will adopt a spherical cap profile defined by a far field contact angle and only in the colloidal region (well below a distance of 0.1 μm), the interfacial profile will deviate because of a competition between the long-range surface and capillary forces, i.e. for radial distances < 100 nm. Keeping constant the contact angle ($\theta_E = 0.1$), we plot spherical cap profiles for submicron sized droplets. Comparison with a calculated local interfacial profile (as described in the

following section) reveals that cap profiles cross the local profile for distances of the order of 40 nm, which is almost of the same order as the droplet contact radius. Now it becomes problematic to imagine a matching between a local profile and a spherical cap profile, as the slopes of the two profiles are very different at the crossing points. Moreover, if one would predict that the contact angle of submicron sized droplets can be described by the modified Young Laplace equation, it is interesting to notice that the calculation of the line tension may become length scale dependent. In fact, for large drops the line tension is calculated from the deviation of the spherical cap profile due to long-range surface forces, which does not change for a drop radius larger than a micron. On the other hand for submicron sized drops the spherical cap profile is strongly affected by the long-range surface interactions and the deviation of the local profile may be due to short-range molecular forces. Indeed, a dependence of the line tension on the wetting perimeter was described by Churaev et al..[25]

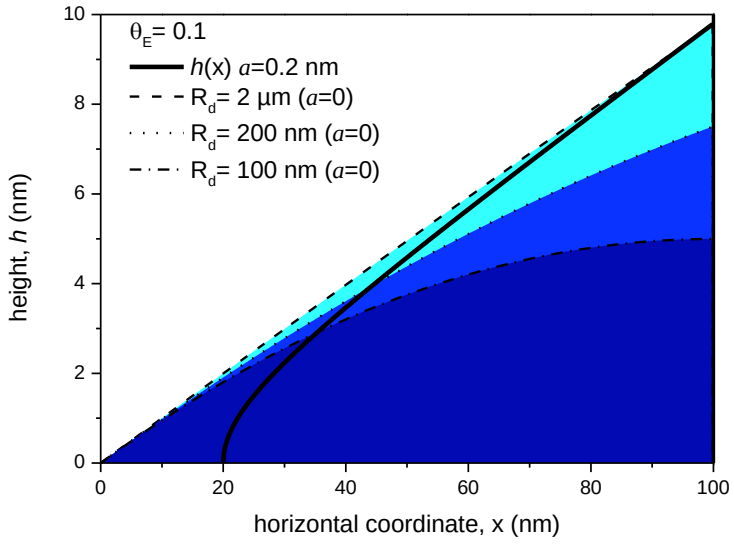

Figure 2. Solid line is an interfacial profile accounting for a repulsive VdW force (a=0.2 nm, θ_E= 0.1, see the text). Three spherical cap profiles for three decreasing droplet radii with θ_E= 0.1 are also shown. At x=0, h=0 for spherical cap profiles (for null VdW forces, a=0).

5. INTERFACIAL PROFILES

Here we focus our description of interfacial profiles for length scales larger than a nanometer and smaller than a micrometer, on cases where the interfacial tensions are not length scale dependent and where short-range molecular forces can be neglected.

The profile of the interface can be calculated by assuming that at equilibrium the chemical potential should be equal along the interface profile. The following equation defines the equilibrium state of a liquid layer of height h :[25]

$$\gamma \Sigma + \Pi(h) = P_0 \qquad \text{Eq. 6}$$

Where γ is the surface tension of the liquid, $\Sigma = \frac{d^2h/dx^2}{[1+(dh/dx)^2]^{3/2}}$ is the local interface curvature, $\Pi(h)$ is the Derjaguin disjoining pressure and the constant P_0 is the capillary pressure of the meniscus. Note that, given the length scale of interest ,gravity is neglected here. In the following we consider the case of nanodroplets, the case of nanobubbles being analogous.

In the colloidal region, the interfacial profile of a droplet can show both positive and negative curvatures, since the Derjaguin disjoining pressure could show a maximum in the range from 1 nm to 1 μm. In fact the interaction between the solid-fluid and fluid-fluid interfaces can be repulsive and attractive depending on the interactions and distance.[26]

Interfacial profiles of droplets accounting for attractive and repulsive VdW forces were calculated and analytical expressions are reported in literature.[27,28,29]

Note that calculations of VdW forces are based on a frequency independent Hamaker constant term, which depends only on the refractive indexes of the media; and a frequency dependent term, which accounts for the spectral properties of the media.[30]

Considering only the effect of VdW forces, the curvature of the interfacial profile is negative for repulsive VdW and positive for attractive VdW forces (see Fig. 3). Note that the sign of the curvature depends on the sign of the second derivative of $h(x)$. Those profiles should be found in every drop and bubble. However, it is very challenging from an experimental view point to measure those profiles without introducing any artifacts.

In Figure 3A we show the spherical cap profile for θ_E = 0.1 rad and R_d = 10 μm together with calculated profiles for repulsive VdW interactions. For the spherical cap profile, when zooming into the nm length scale, the drop shape looks as a straight line of $\tan\theta_E$ slope. Accounting for long-range repulsive VdW forces in equation 6, the drop profile $h(x)$ becomes hyperbolic: [27]

$$Z^2 = -1 + X^2, \qquad \text{Eq. 7}$$

where

$$h = \frac{a}{\theta_E} Z \,, x = \frac{a}{\theta_E^2} X.$$

$a^2 = \frac{A}{6\pi\gamma}$ and a is a characteristic length describing the balance between VdW and interfacial tension terms, A is the repulsive Hamaker constant and γ is the fluid interfacial tension. Note that equation 7 contains two free parameters, a that describes the strength of the VdW force, and θ_E, which describes the far-field equilibrium.

The three profiles are plotted for typical values of a = 0.1, 0.2 and 0.3 nm (e.g. the repulsive Hamaker constant for glass-water-air[5] is 1×10^{-20} J).[30] The deviation of the profile increases, if the characteristic length a increases.

Note that the deviation of the profile is significant for heights lower than a/θ_E, i.e. 1, 2 and 3 nm. Hence, as we discussed in Fig. 2, the hyperbolic profile will match the spherical cap profile for heights of the order of a/θ_E, as one can expect for droplets of micron size or larger. Note that this will be not the case for nanodrops or nanobubbles. In fact for the latter systems the maximum height could be of the same order or even smaller than a/θ_E.

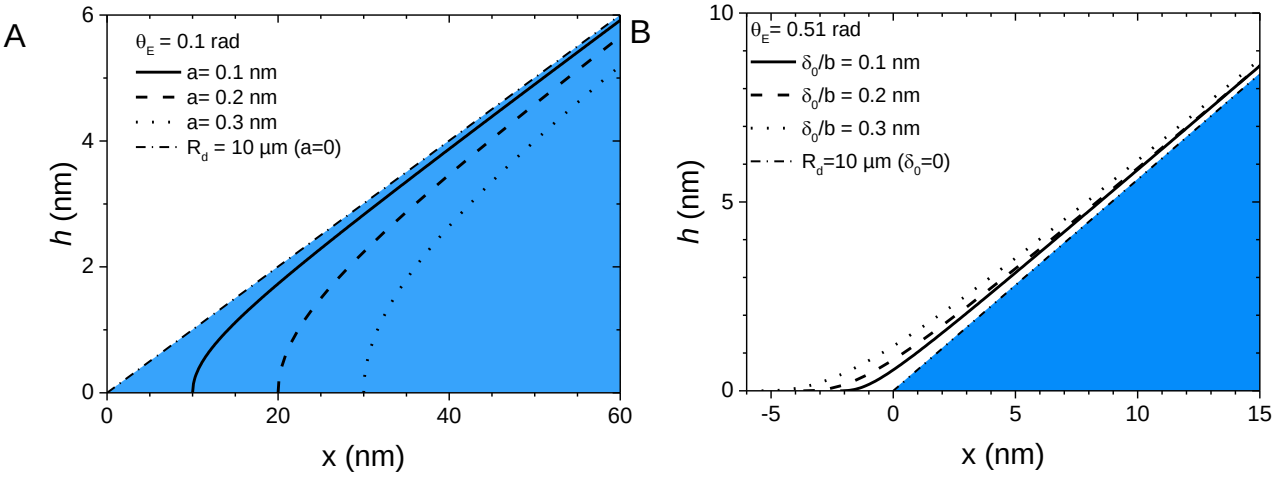

Figure 3. (A) Calculated interfacial profile accounting for repulsive VdW forces with three characteristic lengths *a* = 0.1, 0.2, 0.3 nm and a spherical cap droplet profiles of 10 µm contact radius. (B) Calculated interfacial profile accounting for attractive VdW forces with three characteristic lengths δ_0/b = 0.1, 0.2, 0.3 nm and a spherical cap droplet profiles of 10 µm contact radius. At x=0, *h*=0 for spherical cap profiles (for null VdW forces, *A*=0).

We have also calculated interfacial profiles for attractive Van der Waals forces (Fig. 3B). In this case the square of the slope of the profile is given by:[29]

$$\left(\frac{dZ}{dX}\right)^2 = [(1-2b)^{-1} + (2bZ^2)^{-1}] - 1, \qquad \text{Eq. 8}$$

where

$h = \delta_0 Z\,, x - x_0 = \delta_0 X\,.$

Here δ_0 is a distance defined by: $\delta_0^2 = \frac{bA}{6\pi\gamma}$, and b is related to the equilibrium contact angle by: $\cos\theta_E = 1 - 1/(2b)$. x_0 is a constant, which depends on the boundary condition of the profile.

Profiles are calculated subtracting a baseline of height δ_0, which corresponds to the height of the molecular wetting film coexisting with the meniscus. To calculate the profiles in Fig 3(B), Eq. 8

was solved numerically and in a good approximation can be represented by the analytical function:

$$Z = tan\theta_E \left(X - \sqrt{2b} \arctan\left(\frac{X}{\sqrt{2b}}\right)\right) \qquad \text{Eq. 9}$$

In Fig. 3 we show the interfacial profiles for three typical values of δ_0 (e.g. the attractive Hamaker constant for glass-air-water[5] is 5×10^{-20} J) together with a spherical cap profile for θ_E = 0.51 rad and R_d = 10 μm. As we pointed out, it must be noted that the height of nanodroplets and nanobubbles corresponds to a length, where the interfacial profile is strongly affected by VdW forces. The nanometric droplet or bubble actually exists only in the colloidal region (see Fig. 1), where equation 2 and 5 can not be strictly applied. Hence, it can be argued that if a droplet exists only in the colloidal region and it adopts a spherical-like cap profile, it does not imply that it will adopt the same contact angle as the one defined in the far field, where only capillarity matters.

Here we suggest that the contact angle adopted by the droplet is closely related to the local angle of the interfacial profile, which describes the competition between long-range surface and capillary forces.

Accounting for a disjoining pressure only due to VdW forces of the form: $\Pi(h) = A/6\pi h^3$ one might estimate the contribution of long-range surface and capillary forces on the interfacial profile.[5]

Neglecting the gravity term, the droplet profile obeys to equation 6:[31] $\Sigma + \Pi(h)/\gamma = P_0/\gamma = C_0$.

To find the constant C_0 it is convenient to look at the drop maximum, where the first derivative of the profile is zero.

When the drop maximum height is larger than 0.1 μm, the disjoining pressure decays almost to zero, $\Pi(h_{MAX}) = 0.2$ J/m^3 ≈ 0 ($A/6\pi\gamma h_{MAX}^3 \approx 1/(0.3$ m)) , and $C_0 = P_0/\gamma = 1/R_0$ is the curvature of the drop at the maximum height, i.e. assuming a spherical cap shape and $\theta_L = 0.1$ rad, $1/R_0 = 1/(20$ μm) (see Fig. 4B).

For small droplets the disjoining pressure does not decay close to zero anymore and

$$C_0 = P_0/\gamma = 1/R_0 + A/6\pi\gamma h_{MAX}^3. \qquad \text{Eq. 10}$$

When $h = 1$ nm, $A/6\pi\gamma h_{MAX}^3 \approx 1/(30$ nm) showing that the contribution of the long-range surface force becomes as important as the capillary one for nanodrops and nanobubbles, i.e. assuming a spherical cap shape and $\theta_L = 0.1$ rad, $1/R_0 = 1/(200$ nm) (see Fig. 4B).

.

6. RESULTS AND DISCUSSION

Here, we propose a simple criterion which states that a droplet, whose dimensions are in the colloidal domain, will adopt a spherical cap profile to minimize its area with a contact angle dictated by the local contact angle which accounts for both long-range surface forces and capillarity.

Hence according to this criterion, the contact angle of a nano-sized droplet of height h_{MAX} is equal to the local contact angle of the interfacial profile at the same height (Fig. 4A). The nano-sized droplet and the interfacial profile share the same contact in x, and the droplet contact radius is (see Fig. 4B):

$R_d = h_{MAX} \sin\theta_L / (1-\cos\theta_L)$.

In Fig. 4, two droplets of different heights are shown. Significant differences in contact angles can be observed for droplet radii R_d smaller than 100 nm. Increasing the droplet height, the slope of the interfacial profile varies slowly and approaches the far-field value $\tan\theta_E$.

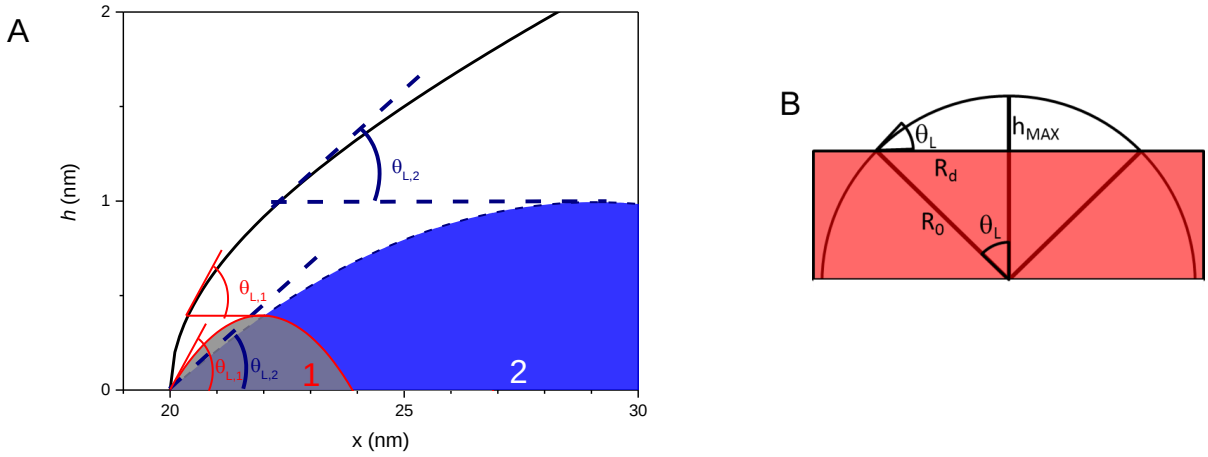

Figure 4. (A) Criterion for the definition of the contact angle for two nanometric droplets. The height of the droplet defines the contact angle in the interfacial profile calculated accounting for VdW forces. The droplet and the interfacial profile share the same contact at h = 0 (here at x=20 nm). (B) Sketch of the contact radius R_d, radius of curvature R_0 and maximum height of a spherical cap shape drop or bubble.

Using the same criterion represented in Fig. 4, in Fig. 5A and 5C we plot the local contact angle θ_L as a function of $R_d = h_{MAX} \sin\theta_L / (1-\cos\theta_L)$ for all calculated profiles. Note that for droplet radius of 50 nm the local contact angle approaches the equilibrium contact angle, while local contact angles dramatically change around droplet radii of about 10 nm.

At this point we would like to compare our calculated data shown in Fig. 5A and 5C with the modified Young-Laplace equation (equation 5), and the linear relation of the cosine of the contact angle with the inverse of the droplet radius.

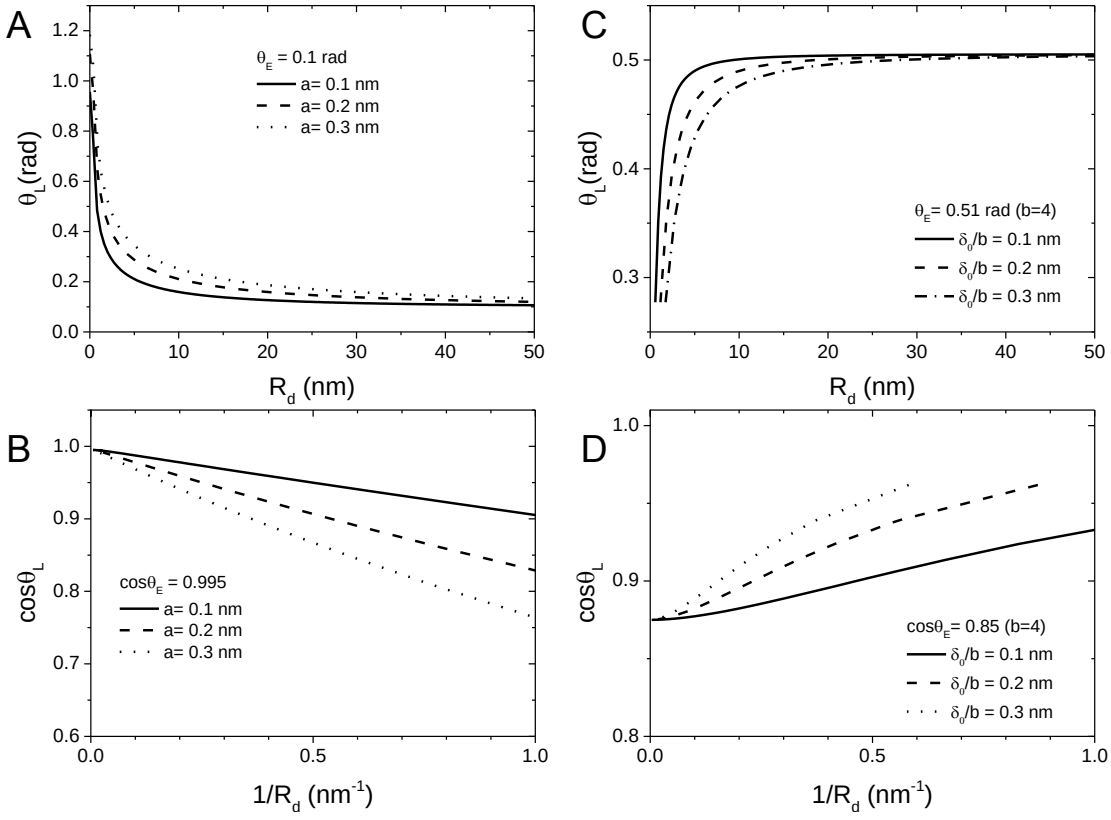

Figure 5. Local contact angles calculated for repulsive (A) and attractive (C) VdW forces as a function of a droplet contact radius defined as $R_d = h_{MAX} \sin\theta_L / (1-\cos\theta_L)$. Cosine of local contact angles calculated for repulsive (B) and attractive (D) VdW forces as a function of the inverse of R_d.

Note that our calculations accounted only for repulsive and attractive VdW forces in the interfacial profile of drops in the mean field. The shapes of the interfacial profiles were calculated using equation 7 and 8. Equation 5 instead assumes that the interfacial profile could be described simply by a constant value line tension defined for macroscopic systems. Hence the underlying physics of our result and the line tension approach are completely different, and we argue, that interpreting the size-dependence of the contact angle in terms of a constant value line tension is not correct.

Just for the sake of comparison, in Fig. 5B and 5D we replotted the data shown in Fig. 5A and 5C as for line tension measurements (equation 5). For repulsive VdW forces, a linear trend of $\cos\theta_L$ with the drop curvature can be observed. From these slopes one would find positive line tensions $k = 6.5 \times 10^{-12}$ N ($a = 0.1$ nm), 1.2×10^{-11} N ($a = 0.2$ nm), 1.7×10^{-11} N ($a = 0.3$ nm) assuming an interfacial tension $\gamma = 72$ mN/m. For attractive VdW forces, the trend of $\cos\theta_L$ with the drop curvature is not linear. Actually, these curves recall the shape of experimental curves reported by Berg *et al* and Checco *et al.*.[7,8] The apparent slopes found fitting the data for attractive VdW forces correspond to negative line tensions $k \approx -6 \times 10^{-12}$ N ($\delta_0/b = 0.1$ nm), -9×10^{-12} N ($\delta_0/b = 0.2$ nm), -1.4×10^{-11} N ($\delta_0/b = 0.3$ nm), assuming an interfacial tension $\gamma = 72$ mN/m.

Those line tension values would agree with reported theoretical and experimental values.[24] Here, positive line tensions correspond to the case of repulsive VdW forces, whereas negative line tensions correspond to attractive VdW forces. In the Supporting Information, we show a comparison of our model with nanobubble and nanodroplet experiments.

As shown in Fig. 4D and in some experiments, the cosine of the droplet contact angle is not linear with the inverse of the droplet radius if the droplet size is nanometric.[7,8] The linear relation could be found only for the modified Young-Laplace equation if drops exist in the far-field. In this case the line tension k can be also calculated theoretically. k is a constant of the system, which represents the energy not accounted for in the bulk and surface terms, when far-field asymptotes can be defined.

For nanometric droplets we can relate the contact angle to the local interfacial profile, which represents the competition of forces acting at the colloidal length scale. Thus, the relation between the droplet contact angle and the droplet size is dictated by the shape of the interfacial profile in the colloidal region. Hence in general, the cosine of the contact angle is not expected to be linear with the droplet curvature, since the form of the disjoining pressure may show local minima and maxima with the distance, and both positive and negative curvatures could be observed (see Figure 6).[25]

Here we suggest an interpretation of experiments performed on droplets and bubbles of decreasing sizes (down to the nanometer scale) as an effect of local contact angle due to long-range surface forces such as long range VdW forces.

7. SUMMARY AND PERSPECTIVES

Finally, for large drops whose sizes are larger than a micron, the contact angle is the equilibrium contact angle θ_E defined by the Young-Laplace equations (eq. 2 and 5). Even for those drops, in the contact line region (at nanometric length scales) local contact angles deviate from θ_E, but this

is a local effect that can be considered negligible. If the droplet height is in the nanoscale the droplet profile will be strongly affected by long-range surface forces. In this context, we propose a simple criterion based on the height of the droplet to describe the change of contact angle.

We believe that the work presented here can stimulate some new discussion in the field of nanodrops and nanobubbles. Theoretical work aiming at describing exact interfacial profiles of nanofluids accounting for different terms of disjoining pressure will surely improve the understanding of contact angle and stability results of nanobubbles and nanodrops.

To conclude, we point out two major results presented here that could be used in future studies. Eq. 10 shows that for nanofluids the capillary pressure depends strongly on the distance and on the Hamaker constant of the system. The latter could possess both signs, which would lead to a strong decrease or increase of the capillary pressure for nanobubbles and nanodrops. This result may help improving theoretical modeling on the gas diffusion of nanobubbles.

We also point out that the stability of nanobubbles may result from the onset of repulsive long-range surface interactions observed when the height of the nanobubble decreases (see Figure 6). This repulsive force prevents the shrinking of the fluid and thus enhances the stability. We can assume that when the height of drops or bubbles is larger than an onset distance h^* ($h > h^*$), the resulting interaction is attractive. In this region, the local contact angle decreases with the decreasing distance (Fig. 5(c)), which agrees with the effective negative line tension values observed in experiments and predictable for attractive VdW forces as in nanobubble systems.[14] Below this onset distance, $h < h^*$, a repulsive VdW or electrostatic interaction may stabilize the fluid against further shrinking (see Figure 6). Repulsive VdW interactions are expected for systems when the static and the frequency dependent terms of the Hamaker constant result in

repulsive values. Repulsive electrostatic interactions for nanobubbles may manifest because of the negative potential of the gas-water and solid-water interfaces.[27]

A clear perspective of this work is to include the contributions of electrostatic, hydrophobic and hydration interactions (together with VdW forces) into the disjoining pressure in order to reinterpret experimental results obtained for nanodrops and nanobubbles.[14]

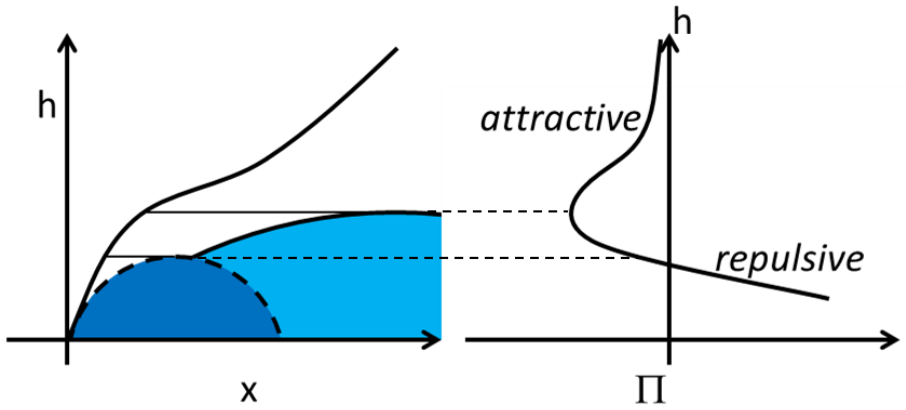

Figure 6. Sketch of an interfacial profile defying the contact angle of two nanodroplets or nanobubbles according to the criterion shown in Fig.4 and the connection with the profile of the disjoining pressure Π(h).

ASSOCIATED CONTENT

Supporting Information. Comparison between the model and experimental results. This material is available free of charge via the Internet at http://pubs.acs.org.

AUTHOR INFORMATION

Corresponding Author

*Antonio.Stocco@umontpellier.fr.

Author Contributions

The manuscript was written through contributions of all authors. All authors have given approval to the final version of the manuscript.

ACKNOWLEDGMENT

We thank Davide Ruffoni, Peter Kralchevski, Ahmed Mourran, Maurizio Nobili, Martin In and Renaud Denoyel for discussion and Labex Chemisyst for financial support. A. S. gratefully acknowledges the Alexander von Humboldt foundation for a research fellowship.

REFERENCES

(1) Gibbs, J. G.; Zhao, Y.-P. P. *Appl. Phys. Lett.* **2009**, *94*, 163104.

(2) Craig, V. S. J. *Soft Matter* **2011**, *7*, 40.

(3) Méndez-Vilas, A.; Jódar-Reyes, A. B.; González-Martín, M. L. *Small* **2009**, *5*, 1366–1390.

(4) Meyer, E. E.; Rosenberg, K. J.; Israelachvili, J. *Proc. Natl. Acad. Sci. U. S. A.* **2006**, *103*, 15739–46.

(5) Israelachvili, J. N. *Intermol. Surf. Forces* **2011**, 205–222.

(6) Kuchin, I. V.; Matar, O. K.; Craster, R. V.; Starov, V. M. *Colloids Interface Sci. Commun.* **2014**, *1*, 18–22.

(7) Berg, J. K.; Weber, C. M.; Riegler, H. *Phys. Rev. Lett.* **2010**, *105*, 076103.

(8) Checco, A.; Guenoun, P.; Daillant, J. *Phys. Rev. Lett.* **2003**, *91*, 186101.

(9) Zhao, B.; Song, Y.; Wang, S.; Dai, B.; Zhang, L.; Dong, Y.; Lü, J.; Hu, J. *Soft Matter* **2013**, *9*, 8837.

(10) Borkent, B. M.; De Beer, S.; Mugele, F.; Lohse, D. *Langmuir* **2010**, *26*, 260–268.

(11) De Gennes, P.-G.; *Rev. Mod. Phys.* **1985**, *57*.

(12) Karpitschka, S.; Dietrich, E.; Seddon, J.; Zandvliet, H.; Lohse, D.; Riegler, H. *Phys. Rev. Lett.* **2012**, *109*, 066102.

(13) Zhang, X. H.; Maeda, N.; Craig, V. S. J. *Langmuir* **2006**, *22*, 5025–35.

(14) Lohse, D.; Zhang, X. *Rev. Mod. Phys.* **2015**, *87*, 981–1035.

(15) Lohse, D.; Zhang, X. *Phys. Rev. E* **2015**, *91*, 031003.

(16) Peng, H.; Birkett, G. R.; Nguyen, A. V. *Adv. Colloid Interface Sci.* **2014**, 3–10.

(17) Weijs, J. H.; Lohse, D. *Phys. Rev. Lett.* **2013**, *110*, 054501.

(18) Kameda, N.; Nakabayashi, S. *Chem. Phys. Lett.* **2008**, *461*, 122–126.

(19) Drelich, J.; Miller, J. *Part. Sci. Technol.* **1982**, *10*, 1–20.

(20) Snoeijer, J. H.; Andreotti, B. *Phys. Fluids* **2008**, *20*, 057101.

(21) Snoeijer, J. H.; Andreotti, B. *Annu. Rev. Fluid Mech.* **2013**, *45*, 269–292.

(22) Schimmele, L.; Naplórkowski, M.; Dietrich, S. *J. Chem. Phys.* **2007**, *127*.

(23) Drelich, J. In *Colloids and Surfaces A: Physicochemical and Engineering Aspects*; 1996; Vol. 116, pp. 43–54.

(24) Pompe, T.; Herminghaus, S. *Phys. Rev. Lett.* **2000**, *85*, 1930–1933.

(25) Churaev, N. .; Starov, V. .; Derjaguin, B. . *J. Colloid Interface Sci.* **1982**, *89*, 16–24.

(26) Kuchin, I. V.; Matar, O. K.; Craster, R. V.; Starov, V. M. *Colloids Interface Sci. Commun.* **2014**, *1*, 18–22.

(27) De Gennes, P. G.; Hua, X.; Levinson, P. *J. Fluid Mech.* **1990**, *212*, 55–63.

(28) Wayner, P. . *J. Colloid Interface Sci.* **1980**, *77*, 495–500.

(29) Wayner, P. . *J. Colloid Interface Sci.* **1982**, *88*, 6–7.

(30) Bergström, L. *Adv. Colloid Interface Sci.* **1997**, *70*, 125–169.

(31) Sharma, A. *Langmuir* **1993**, 3580–3586.

(32) Chaplin, M. *Water* **2009**, *1*, 1–28.

Insert Table of Contents Graphic and Synopsis Here